

Data-Driven Network Neuroscience: On Data Collection and Benchmark

David Tse Jung Huang^{1*}, Sophi Shilpa Gururajapathy^{2*}, Yiping Ke²,
Miao Qiao¹, Alan Wang^{3,4,5}, Haribalan Kumar⁶, and Yunhan Yang¹
partially for the Alzheimer's Disease Neuroimaging Initiative[†]

¹School of Computer Science, The University of Auckland, New Zealand

²School of Computer Science and Engineering, Nanyang Technological University, Singapore

³Auckland Bioengineering Institute, The University of Auckland, New Zealand

⁴Faculty of Medical and Health Sciences, The University of Auckland, New Zealand

⁵Centre for Brain Research, The University of Auckland, New Zealand

⁶General Electric Healthcare Magnetic Resonance, Australia & New Zealand

{dtj.huang, miao.qiao, alan.wang, yunhan.yang}@auckland.ac.nz

{sophi.sg, ypke}@ntu.edu.sg

Haribalan.Kumar@ge.com

Abstract

This paper presents a comprehensive and quality collection of functional human brain network data for potential research in the intersection of neuroscience, machine learning, and graph analytics. Anatomical and functional MRI images of the brain have been used to understand the functional connectivity of the human brain and are particularly important in identifying underlying neurodegenerative conditions such as Alzheimer's, Parkinson's, and Autism. Recently, the study of the brain in the form of brain networks using machine learning and graph analytics has become increasingly popular, especially to predict the early onset of these conditions. A brain network, represented as a graph, retains richer structural and positional information that traditional examination methods are unable to capture. However, the lack of brain network data transformed from functional MRI images prevents researchers from data-driven explorations. One of the main difficulties lies in the complicated domain-specific preprocessing steps and the exhaustive computation required to convert data from MRI images into brain networks. We bridge this gap by collecting a large amount of available MRI images from existing studies, working with domain experts to make sensible design choices, and preprocessing the MRI images to produce a collection of brain network datasets. The datasets originate from 5 different sources, cover 3 neurodegenerative conditions, and consist of a total of 2,642 subjects. We test our graph datasets on 5 machine learning models commonly used in neuroscience and on a recent graph-based analysis model to validate the data quality and to provide domain baselines. To lower the barrier to entry and promote the research in this interdisciplinary field, we release our brain network data <https://doi.org/10.17608/k6.auckland.21397377> and complete preprocessing details including codes.

*Equal contribution

[†]Part of the data used in preparation of this article were obtained from the Alzheimer's Disease Neuroimaging Initiative (ADNI) database (adni.loni.usc.edu). As such, the investigators within the ADNI contributed to the design and implementation of ADNI and/or provided data but did not participate in the analysis or writing of this report. A complete listing of ADNI investigators can be found at: http://adni.loni.usc.edu/wp-content/uploads/how_to_apply/ADNI_Acknowledgement_List.pdf

1 Introduction

Neuroscience studies the brain and its impact on human behaviour and cognitive functions by examining brain structures and functions. It unveils the principles and mechanisms underlying complex brain function and cognition of not only the normal brain, but also brains with neurological, psychiatric, and neurodevelopmental conditions. Resting-state functional magnetic resonance imaging (rs-fMRI) is a non-invasive technique for examining functional connectivity of the brain by monitoring changes associated with blood flow, as blood-oxygen-level-dependent (BOLD) signals, to identify areas of increased or decreased neuronal activity [21]. Traditionally, the process of examining the brain heavily relied on domain experts to manually curate and analyze data from brain scans. The process is usually time-consuming which limits the scale of the study.

Recently, there is a rapid expansion in the size, scope and complexity of neural data acquired from large portions of nervous systems and spanning multiple levels of organization. Combined with computational advancements in machine learning and graph analytics, this joint progress is driving further research efforts in the area of network neuroscience [11]. Network neuroscience is a branch of neuroscience that understands the structure and function of the human brain through the paradigm of graph theory. As acquired neural data becomes more complex, representing and modelling the brain in graph form becomes desirable to drive further scientific research and discovery. In network neuroscience, the brain is modelled as a graph with neurons/brain regions as nodes and their connections/interactions as edges, which is called a brain network. This form of representation is able to capture richer structural and positional information that traditional manual examinations are incapable of capturing. Examples include dynamic patterns of neural signaling and communication associated with spontaneous and task-evoked brain activity, synaptic connections among brain areas, and interactions among brain systems and the environment in the course of behavior [7].

Graph-based models have successes in many domains such as social science [47], biology [29], and computer vision [28], with practical tasks including community detection [20], graph classification [15], link prediction [52], etc. These models have great potential in neuroscience as brains are natural networks both functionally and structurally. A community in brain networks could represent areas of co-activation which could be weakened for brains suffering from neurodegenerative conditions [30]. Graph classification can help identify subjects at different stages of neurological diseases. However, the lack of available brain network datasets set barriers to in-depth methodological research.

The conversion of brain networks from MRI scans is non-trivial and requires intensive domain inputs. The process has two main stages. First, raw MRI images need to be preprocessed and quality controlled to ensure the image quality for subsequent tasks. It involves a large number of pipeline steps, including motion correction, realigning, field unwarping, normalization, bias field correction, and brain extraction. In addition, different preprocessing choices made in different studies introduce a large variance in output images. Second, preprocessed MRI images are parcellated into regions-of-interest (ROIs) as nodes, with the co-activation between ROIs as weighted links. Typically, each study selects a single parcellation scheme to generate a fixed set of nodes for all subjects in the study, while the effect of different choices of parcellation schemes remains largely unexplored. Each generated brain network contains a weighted adjacency matrix and a feature matrix. The former characterizes the connectivity between brain regions, and the latter captures the attributes of brain regions in terms of the aggregated BOLD signals.

The conversion steps pose several challenges that are the current roadblocks for researchers to have adequate access to brain networks. (1) Domain knowledge in neuroimage preprocessing is required to select and guide the proper pipeline and tools used; (2) High computational cost in both image processing and graph extraction; and (3) Large-scale imaging studies have a complex setup with multi-site, multi-scanner, and multiple acquisition protocols. This paper aims to bridge the gap in publicly accessible brain network datasets by making more data available. We believe that the release of this collection of brain networks would promote research in the interdisciplinary field of network neuroscience, machine learning, and graph analytics, and drive further advances in graph-based studies and clinical studies such as the classification and detection of neurodegenerative conditions.

The main contributions are highlighted below.

1. We release a functional brain network collection to the public at a large scale. The collection originates from 5 raw MRI image sources well recognized in neuroscience, covers 3

neurodegenerative conditions and consists of ABIDE (N=1025), ADNI (N=1327), PPMI (N=209), and two other sources totalling to 2,642 subjects.

2. We worked closely with domain experts to make sensible design choices on the preprocessing pipeline, the tools to be used, as well as the parameters to be chosen. We then convert the collection of raw MRI images to brain networks, using a uniform data processing pipeline such that the variance in the output networks could be minimized.
3. We tested the datasets on several base machine learning models and one recent graph-based model. It demonstrates that the data quality is not compromised by the conversion process. As these models are commonly used in neuroscience, the results also serve as domain baselines for subsequent research.

2 Related Work

We discuss related work in the preprocessing of MRI images and their public availability. The most relevant work to our study is the Preprocessed Connectomes Project (PCP) [13], which is an initiative to preprocess part of the raw MRI images in the International Neuroimaging Data-sharing Initiative (INDI) database and make *the preprocessed neuroimages* publicly available. Within PCP, one relevant dataset that has gone through functional preprocessing pipelines is the ABIDE dataset, which studies Autism. Our study includes two additional clinical conditions of interest, Alzheimer’s and Parkinson’s Disease, extracts brain networks under different parcellation schemes and wraps the whole conversion process from raw MRI images to brain networks in a holistic manner. We focus on making functional brain connectivity in the form of brain networks publicly available, using the state-of-the-art functional preprocessing pipeline, fMRIPrep, which is not available from PCP. Compared to other preprocessing tools, fMRIPrep introduces less uncontrolled spatial smoothness [16].

Recently, the research of network neuroscience combined with machine learning models and graph-based analysis has attracted increasing attention [19]. Most recent studies along this line of research [9, 45, 33, 25, 30] work on the ABIDE dataset with the preprocessed images provided by PCP. They generate brain networks and apply machine learning models to perform connectivity analysis. In [38, 1], a collection of graph datasets was released, which includes 3 brain network datasets (KKI, OHSU, and Peking_1) originally introduced in [40]. These datasets consist of binarized graphs with a small number of sample sizes ($N \approx 80$) for Attention Deficit Hyperactivity Disorder (ADHD). A single data-driven parcellation scheme [14] is used in generating these datasets. In [30], the ABIDE dataset is also released as binarized graphs. In this work, we aim to release a collection of brain networks that include datasets with both large and small sample sizes, and with a variety in clinical conditions and brain parcellation schemes. We also release the codes of the entire processing pipeline, which keeps future efforts in refining the pipeline and/or enriching the collection open.

3 Dataset Sources: Raw Neuroimages

This section describes our selected sources of raw neuroimages and their selection and acquisition settings. Table 1 summarizes our datasets and the generated brain networks. The number of nodes in each brain network is determined by the parcellation scheme (detailed in Section 4.4) and therefore the number of non-zero edges varies under different parcellations. We focus on examining functional connectivity of the brain using resting-state functional magnetic resonance imaging (rs-fMRI), which is shown to be effective in the identification of brains with neurodegenerative conditions [21]. Each rs-fMRI image needs to be accompanied with a structural T1-weighted (T1w) image acquired from the same subject in the same scan session. The T1w image provides structural details of the subject’s brain; when used together with rs-fMRI, it helps to extract the brain mask and perform image alignment and normalization of the BOLD time series, such that the preprocessed images can achieve a better quality. The same requirement exists in other pipelines such as DPARSF [51].

Autism Brain Imaging Data Exchange (ABIDE) The ABIDE initiative has aggregated functional and structural brain imaging data collected from laboratories around the world to support the research in understanding the neural bases of autism. Autism Spectrum Disorder (ASD) is characterized by stereotyped behaviors such as irritability, hyperactivity, depression, and anxiety. Its symptoms develop as early as 1-2 years of age [34] and clinical diagnoses are possible by 2-3 years of age [44]. Subjects are classified into typical controls or those suffering from ASD.

Table 1: Summary of our datasets and the generated brain networks. Each subject has a graph (brain connectivity network) generated under each Parcellation Method (PM), e.g., AAL, HarvardOxford (HO), Schaefer, k-means and Ward Clustering (see Table 2 for details). The number of nodes of a graph generated under a PM is the number of ROIs of the PM. We call an edge a non-zero edge if its weight has absolute value $> 10^{-2}$. The number of features is the length of the BOLD signals.

Dataset	Condition	# Graphs (# Subj)	# Class	Avg # Non-Zero Edges under PM (# Nodes)					Avg # of Features
				AAL (116)	HO (48)	Schaefer (100)	k-means (100)	Ward (100)	
ABIDE	Autism	1025	2	6402	1112	4811	4698	4729	201
ADNI	Alzheimer	1327	6	6447	1112	4824	4734	4715	344
PPMI	Parkinson	209	4	6512	1122	4866	4795	4684	198
TaoWu	Parkinson	40	2	6481	1116	4846	4724	4766	239
Neurocon	Parkinson	41	2	6455	1114	4830	4677	4779	137

Alzheimer’s Disease Neuroimaging Initiative (ADNI) ADNI [4, 3, 50] is a longitudinal multisite study designed to develop clinical, imaging, genetic, and biochemical biomarkers for the early detection and tracking of Alzheimer’s Disease (AD). AD is a progressive neurologic disorder that causes the brain to shrink and brain cells to die and is the most common cause of dementia that affects a person’s ability to function independently. ADNI data used in this study were obtained from the ADNI database (adni.loni.usc.edu) which was launched in 2003 as a public-private partnership, led by Principal Investigator Michael W. Weiner, MD. The primary goal of ADNI has been to test whether serial MRI, positron emission tomography (PET), other biological markers, and clinical and neuropsychological assessment can be combined to measure the progression of mild cognitive impairment (MCI) and early Alzheimer’s disease (AD). For up-to-date information, visit www.adni-info.org. We included subjects from 6 different stages of AD, from cognitive normal (CN), significant memory concern (SMC), mild cognitive impairment (MCI), early MCI (EMCI), late MCI (LMCI) to Alzheimer’s disease (AD) [8].

Parkinson’s Progression Markers Initiative (PPMI) PPMI aims to identify biological markers of Parkinson’s risk, onset and progression. Parkinson’s disease is a progressive nervous system disorder that mainly affects movement [37]. Its symptoms start gradually, sometimes starting with a barely noticeable tremor in just one hand. The study is ongoing and contains multimodal, multi-site MRI images similar to the ADNI study [31]. PPMI dataset contains subjects in 4 classes: normal control, scans without evidence of dopaminergic deficit (SWEDD), prodromal, and Parkinson’s disease (PD).

TaoWu and Neurocon TaoWu and Neurocon datasets are released by ICI [6] and are two of the earliest image datasets released for Parkinson’s. The datasets consist of age-matched subjects captured using a single machine and on a single site. We include these two datasets in our collection as they could be used in studies that aim to minimize or contrast the variability introduced from different image acquisition settings. It includes normal controls and patients labelled with PD. Neurocon and TaoWu label patients with a diagnosis of PD who have been under treatment (most under levodopa) as PD. PPMI’s PD definition involves patients with a diagnosis of PD for two years or less and who are not taking PD medications. Under these definitions, Neurocon and TaoWu are more similar when compared to PPMI. It is worth noting that while these two have similar scanning protocols, they used different scanners (with TaoWu being higher in resolution). In [6], the authors compared these scans and argued that they can be treated similarly. We believe there could be more such explorations with the data available, which is one of the main reasons why we want to release this collection.

4 From MRI Images to Brain Networks: Design Choices

We adopt the common functional processing steps in network neuroscience [17] to convert raw MRI images (rs-fMRI and T1w) into brain networks, as depicted in Figure 1. Our preprocessing steps and choices were guided by domain experts. They have provided advice/feedback on the selection of images from the data sources, our choice of using the state-of-the-art fMRIPrep pipeline, parcellation strategies, quality check of fMRIPrep outputs, and the selection of confounds. First, raw MRI images are collected based on the selection criteria (Section 4.1). The images are then converted into BIDS

format and preprocessed using fMRIPrep (Sections 4.2 and 4.3). Preprocessed data is then parcellated into different regions-of-interest (Section 4.4). Finally, the connectivity matrix and the feature matrix are extracted and form the brain network (Section 4.5).

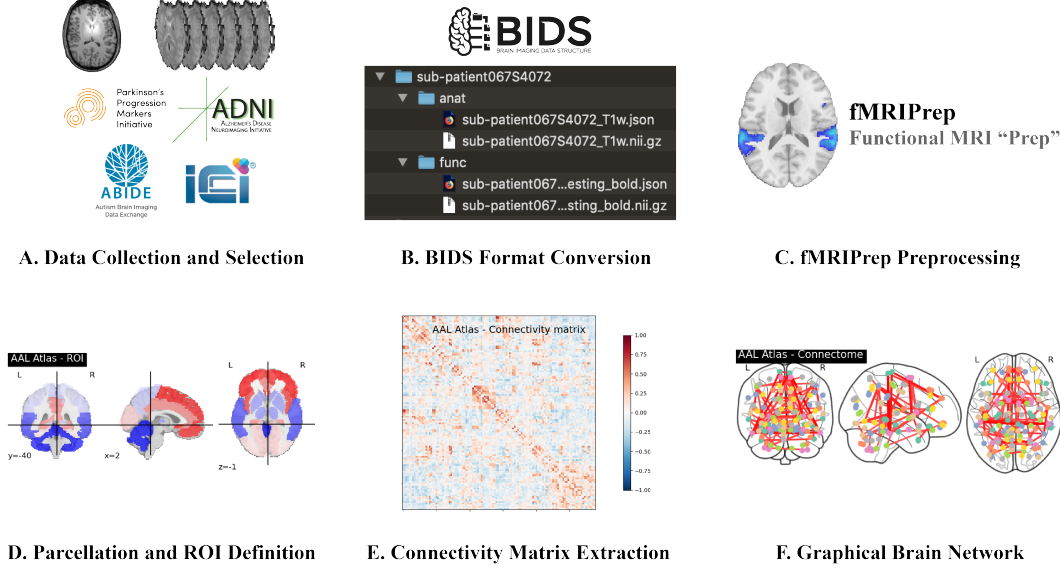


Figure 1: Brain Network Construction Pipeline

4.1 Data Collection and Selection Criteria

As our selected data sources involve multi-site, multi-scanner images, not all images contained within each data source are included in our study. We filter the subjects based on the availability, validity, and quality of our required MRI image types.

For ABIDE, TaoWu, and Neurocon, the original source images were already collated with 1 raw rs-fMRI image paired with 1 T1w image for each subject. We included all subjects provided by the data source except for those that had quality issues. A subject has quality issues if it has an incomplete image (*i.e.*, not containing the full brain) and/or damaged data (*i.e.*, with error reported by any subsequent preprocessing steps). Available metadata of each subject from the source is included in our collection, such as age and gender. We note that for ADNI, our released data contains 6% more females than the original ADNI data. For all other datasets, the gender distributions of our datasets closely match those of the original data sources.

For longitudinal study data sources, ADNI and PPMI, it is possible that some subjects have had multiple scans over the course of several years. Depending on the scanning protocol for the study, different types of images were taken at various times (*e.g.* baseline, 1 year follow-up, 2 year follow-up, etc.). The baseline study (the first scan) is usually the most comprehensive one that would cover a wide range of modalities. Thus, as suggested by our domain experts, we consider the baseline study which is likely to be the set of scans with both an rs-fMRI image and a T1w image taken on the same date. In the case that multiple rs-fMRI and T1w scans exist, we selected the first available one.

For validity, we examined each image manually to make sure the images conformed to their labels in the database and did not have obvious data format issues for preprocessing. We had to check this manually because the image databases often had inconsistent labeling.

In our collection, ABIDE, ADNI, and PPMI are multi-site neuroimaging sources. Therefore, data harmonization may be considered to allow a more reliable joint analysis. In our preprocessing, we did not apply data harmonization techniques to these datasets because of the following reasons: (1) for fMRI connectivity, there is no well-grounded harmonization method for benchmark; (2) even though no fMRI connectivity harmonization was applied, [39] has shown that fMRI connectivity still has some good repeatability; (3) the site and scanner information are available and researchers have the flexibility of performing harmonization based on our data collection for further analysis.

Table 2: Parcellation Methods

Name	# ROIs	Generation Method
AAL [48]	116	Delineated with respect to anatomical landmarks by following the sulci course in the brain
HarvardOxford [36]	48	Created by subdividing neocortex by topographic criteria into 48 parcellation units corresponding to the principal cerebral gyri
Schaefer [46]	100	Automatic using gradient-weighted Markov Random Fields (gwMRF) to group similar fMRI regions
<i>k</i> -means Clustering [35, 2]	100	Top-down clustering algorithm that partitions voxels into non-overlapping predefined number of regions
Ward Clustering [49, 2]	100	Bottom-up hierarchical clustering algorithm that agglomerates together voxels progressively into regions

4.2 BIDS Conversion

Raw MRI images are typically in the Digital Imaging and Communications in Medicine (DICOM) format. DICOM images are then converted to the Neuroimaging Informatics Technology Initiative (NIfTI) format using `dcm2niix` [32], which includes a JSON that details various imaging parameters such as scanner model, magnetic field strength, flip angle, slice timing, echo time and repetition time. The NIfTI and JSON files are then organized into a folder hierarchy with a precise naming convention known as Brain Imaging Data Structure (BIDS) [24]. After conversion, BIDS formatted data can be applied to preprocessing pipelines in a highly reproducible and transparent manner.

4.3 fMRIPrep Preprocessing

BIDS compliant datasets are then preprocessed using fMRIPrep [16], a state-of-the-art tool for preprocessing fMRI. fMRIPrep performs basic processing steps (coregistration, normalization, noise component extraction, skull stripping, etc.) and uses a combination of tools from well-known software packages, including FMRIB Software Library (FSL) [26], Analysis of Functional NeuroImages (AFNI) [12], Advanced Normalization Tools (ANT) [5] and FreeSurfer [18]. This pipeline was designed to use the best software implementation for each step of preprocessing. fMRIPrep can be installed via container technologies such as docker or singularity. fMRIPrep automates the pipeline by using the scanner outputs from the images (e.g., slice timing correction parameters are taken automatically from the scanner outputs of the original image data). Therefore, the user does not need to specify these parameters manually. fMRIPrep can be configured to include or exclude specific workflow steps, such as ignoring slice timing. We followed the default automatic fMRIPrep workflow with surface reconstruction enabled. No further modifications to the settings were made as the default workflow met our expectations for a functional preprocessing pipeline. As part of our validation process of fMRIPrep, we have passed the preprocessed images over to our MRI imaging experts: they have carefully examined the outputs to ensure the data quality. fMRIPrep outputs conform to the BIDS Derivatives specification for compatibility and include the preprocessed BOLD images and the confounds file, which records fluctuations during MRI data acquisition, also known as nuisance regressors. fMRIPrep is computationally expensive. In our case, one run on one subject of fMRIPrep using 8 threads on an Intel(R) Core(TM) i9-10940X CPU@3.30GHz took on average 4-5 hours.

4.4 Parcellation Strategies

Parcellation helps to define distinct regions in the brain known as region-of-interest (ROI). The parcellation step takes in these two outputs from fMRIPrep for each subject to generate the parcellations: the preprocessed BOLD image and the confounds file. We adopted the standard 9 parameters (9P) confounds setting widely used in functional connectivity studies [22, 23] for de-noising: white matter, cerebrospinal fluid, global signal, and the 6 rigid-body motion parameters for rotation and translations at x, y and z axes. To parcellate the brain, we selected a list of methods that covers both atlas-based and clustering-based methods frequently used in the domain. A summary of these methods is given in Table 2. An example of the ROIs extracted by these methods is shown in Figure 2.

Brain regions partitioned through pre-defined regions are Atlas-based parcellations. We selected from the most commonly used ones: AAL, HarvardOxford, and Schaefer. They are generated using distinct strategies, giving us a better coverage of ROIs parcellated with different brain features.

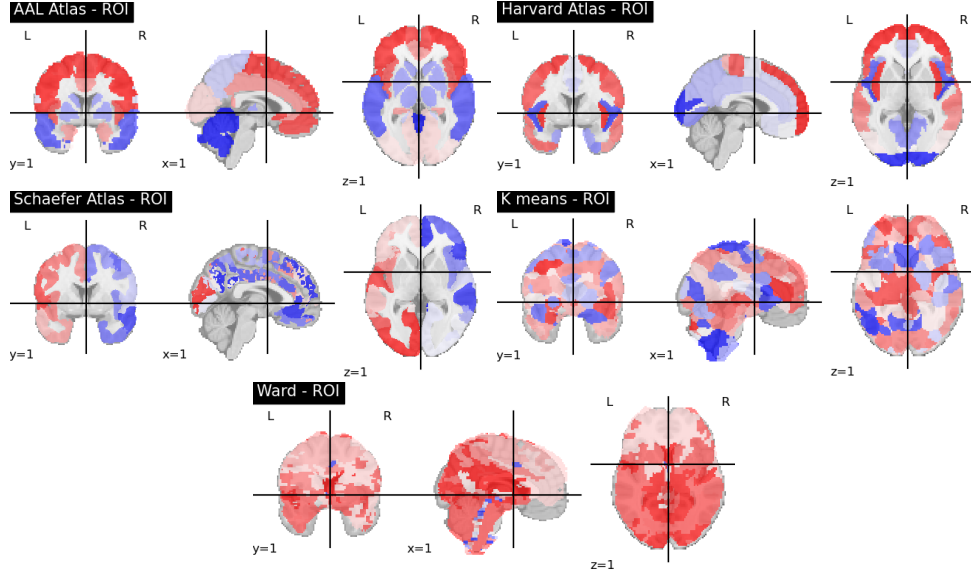


Figure 2: Visualization of ROIs Extracted (Color Variations Denote Unique Regions)

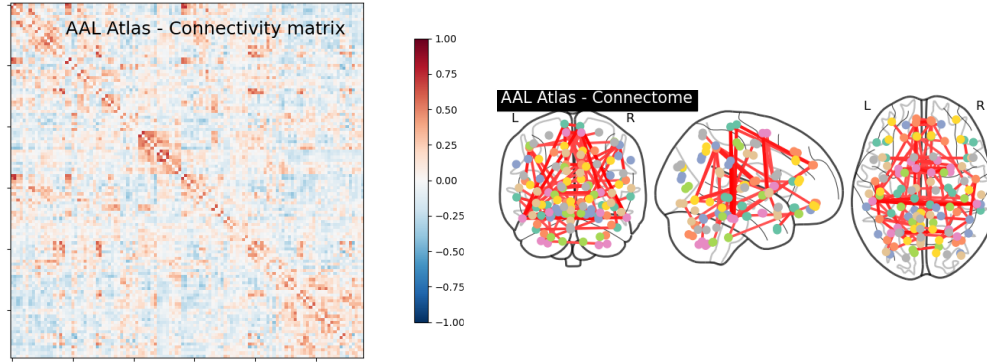


Figure 3: Example Connectivity Matrix (left) and Glass Brain Connectome (right)

Clustering-based parcellations partition the brain by computing the similarity in the BOLD signals between voxels and performing clustering on the voxels based on the similarities. Each subject directly generates its own set of ROIs. k -means and Ward clustering are the two methods used in the domain. We included them and set the number of ROIs as 100, which is close to the predefined value in atlas-based methods. Our datasheet in the Supplementary details the file format and output files.

4.5 Brain Network Extraction

The BOLD signals from parcellated ROIs are used to compute the connectivity matrix of the brain network. The matrix captures functional relationships between parcellated regions and reflects their co-activations. Connectivity matrix is extracted using a built-in function of Nilearn [2] called ConnectivityMeasures [54]. It takes 2 inputs, BOLD signals of the brain regions and the connectivity metric (*e.g.*, correlation). The former is obtained by averaging the BOLD signals of all the voxels lying in the same ROI. An example of a connectivity matrix is shown in Figure 3 left. Among existing connectivity measures (correlation, covariance, partial correlation, etc.), correlation is used by a majority of graph-based neuroscience research [30, 33, 41]. Thus, in our released collection, we select correlation as the connectivity measure and make the fully weighted matrices available without performing any thresholding on the correlation values. For the practitioners who are interested in alternative measures, we have uploaded preprocessed images and our matrix generation code as part of our collection, which enables the researchers to generate their own matrices based on their desired measure. In addition, we have included a datasheet for this data collection in our Supplementary which details our outputs and file formats. The connectivity matrix can be represented equivalently

as a glass brain connectome. An example connectome plot on the AAL atlas is shown in Figure 3 right. The connectome plot shows 1% of brain functional connectivities for visualization.

The brain network constructed by this pipeline has the set of ROIs as nodes and their co-activations (measured as Correlation) as edges. Each brain network is represented by a weighted adjacency matrix and a feature matrix. The former is the connectivity matrix extracted and the latter stores the BOLD signals of ROIs. Such brain networks can be readily used by existing graph-based models.

5 Data Quality Assessment and Baseline Comparisons

To assess if the graph representation maintains the data quality from neuroimages, we test our brain network data collection on standard machine learning models typically used in neuroscience as baseline models in Section 5.1. The aim is to establish a baseline study on this data collection. We focus on the classification task and follow the convention in the domain [9, 25] to vectorize the input connectivity matrices by flattening them. The data is split to 80:20 for training and testing and 5-fold cross-validation is performed. We then test on a recent graph-based analysis on functional networks [30] in Section 5.2 to further validate the quality of our data.

5.1 Learning Models and Results

We select five baseline machine learning models for this study: Logistic Regression (LR), Gaussian Naive Bayes (NB), Support Vector Machine Classifier (SVC), k -Nearest Neighbours (kNN), and Random Forest (RF). Our rationale for using these standard models as baselines is that they are commonly used for classification problems in brain functional analysis [33, 53, 27, 55]. Some recent studies also build upon these standard models for functional connectivity analysis. In [33], the authors designed their model based on SVC and compared it against its standard version. In [53], the authors experimented with LR, kNN, Neural Network, Decision Tree, Random Forest, and SVMs; most of which are also used in our study. In [27], Random Forest was used, and in [55], Naïve Bayes was used. Therefore, we believe that reporting results on these standard models could serve as nice domain baselines for future studies. The implementation from the scikit-learn library [42, 10] is used. In addition, we used Grid Search for model selection. Details on model hyperparameters and Grid Search are provided in the Supplementary.

Table 3 reports the classification accuracy on the datasets using different parcellation methods. We report the best accuracy for each model. We observe that in most cases, the overall accuracy falls within the range of 60% to 70%. This is relatively consistent with the results reported in previous studies [30, 9, 45, 33, 25], despite some differences in data filtering and preprocessing. With respect to parcellation methods, we observe that atlas-based methods in general outperform clustering-based methods. For example, in ABIDE and ADNI, there is an approximately 5%-10% difference in performance across the 5 methods when comparing atlas-based methods vs. clustering-based methods. This is likely due to the effects from some randomness in the clustering process, *e.g.*, initial centroid selection in k -means. Among different learning models, the more sophisticated models, SVC and RF, perform better in most cases. This also explains why SVCs are commonly used as baseline models [30, 33].

There are several strategies and extensions that can be done to further improve these results, such as: adding a feature selection step and/or developing a more targeted learning model. Adding a feature selection step can involve using strategies such as PCA to reduce the feature space or selecting a subset of edges to use in prediction as opposed to using all edges. Sparsity-based manipulations [43] such as binarizing the edges based on a percentile threshold are also commonly performed. More recently, there have been studies that incorporate graph-based methods, such as dense sub-graphs [30], to use as features instead. Developing a more targeted learning model can involve making extensions to existing baseline models, such as SVCs with different kernel functions [33]. By releasing brain networks in the form of fully weighted matrices in this collection, we aim to enable future research that utilizes our data to have the flexibility of choosing sparsity manipulations and/or feature selection methods that better suit their problem. Graph representations further create the potential for the study of graph-based models in neuroscience. With the results presented here on existing models, they could serve as domain baselines for subsequent research.

Table 3: Classification Accuracy (mean \pm standard deviation)

ABIDE					
	AAL	HarvardOxford	Schaefer100	k-means100	Ward100
Logistic Regression	63.9 \pm 3.3	62.7 \pm 2.5	65.0 \pm 4.6	50.6 \pm 4.8	51.6 \pm 1.4
Naïve Bayes	60.7 \pm 5.0	59.8 \pm 5.7	62.2 \pm 6.9	50.2 \pm 5.1	54.6 \pm 2.1
SVC	66.5 \pm 3.0	64.3 \pm 2.6	65.4 \pm 5.9	52.4 \pm 0.2	55.6 \pm 2.1
kNN	60.6 \pm 1.7	57.3 \pm 2.6	59.6 \pm 2.6	53.1 \pm 1.5	48.2 \pm 0.4
Random Forest	64.1 \pm 4.0	62.3 \pm 4.2	63.6 \pm 3.8	52.3 \pm 1.5	55.1 \pm 3.3
ADNI					
	AAL	HarvardOxford	Schaefer100	k-means100	Ward100
Logistic Regression	74.9 \pm 2.2	67.3 \pm 2.6	71.1 \pm 2.9	54.2 \pm 2.2	56.1 \pm 2.2
Naïve Bayes	62.1 \pm 3.1	61.5 \pm 2.6	57.7 \pm 2.4	41.0 \pm 3.0	53.3 \pm 3.4
SVC	76.6 \pm 1.7	72.4 \pm 2.0	74.3 \pm 2.3	61.7 \pm 0.1	61.9 \pm 0.6
kNN	67.5 \pm 3.5	68.8 \pm 2.2	67.8 \pm 1.6	44.9 \pm 10.8	50.6 \pm 9.4
Random Forest	66.9 \pm 1.3	67.4 \pm 1.8	65.9 \pm 1.4	61.8 \pm 0.2	61.8 \pm 0.2
PPMI					
	AAL	HarvardOxford	Schaefer100	k-means100	Ward100
Logistic Regression	56.4 \pm 2.1	57.9 \pm 5.1	56.4 \pm 3.0	59.3 \pm 5.1	58.9 \pm 4.7
Naïve Bayes	61.0 \pm 7.1	60.4 \pm 8.3	61.9 \pm 7.4	59.4 \pm 6.4	62.3 \pm 7.4
SVC	65.1 \pm 3.3	64.6 \pm 2.2	62.7 \pm 3.2	61.3 \pm 4.0	62.2 \pm 3.6
kNN	54.5 \pm 3.4	59.3 \pm 3.4	58.9 \pm 7.4	61.7 \pm 3.6	61.7 \pm 2.6
Random Forest	66.1 \pm 2.5	65.1 \pm 2.2	64.6 \pm 1.6	61.2 \pm 3.2	62.7 \pm 4.3
TaoWu					
	AAL	HarvardOxford	Schaefer100	k-means100	Ward100
Logistic Regression	82.5 \pm 12.7	72.5 \pm 12.2	70.0 \pm 12.7	42.5 \pm 10.0	45.0 \pm 17.0
Naïve Bayes	61.5 \pm 19.0	61.0 \pm 19.5	64.0 \pm 18.1	31.5 \pm 10.1	36.5 \pm 19.0
SVC	85.0 \pm 9.4	75.0 \pm 7.9	70.0 \pm 12.7	50.0 \pm 0.0	52.5 \pm 12.2
kNN	60.0 \pm 14.6	67.5 \pm 10.0	62.5 \pm 20.9	52.5 \pm 5.0	50.0 \pm 0.0
Random Forest	72.5 \pm 12.2	70.0 \pm 15.0	75.0 \pm 15.8	62.5 \pm 11.2	57.5 \pm 10.0
Neurocon					
	AAL	HarvardOxford	Schaefer100	k-means100	Ward100
Logistic Regression	63.1 \pm 11.8	63.3 \pm 11.3	63.3 \pm 1.7	63.3 \pm 1.7	63.3 \pm 1.7
Naïve Bayes	60.0 \pm 14.1	60.4 \pm 14.8	59.1 \pm 12.1	56.4 \pm 14.0	59.1 \pm 12.9
SVC	65.8 \pm 4.9	63.3 \pm 1.7	68.3 \pm 5.7	63.3 \pm 1.7	63.3 \pm 1.7
kNN	65.6 \pm 6.1	63.3 \pm 8.1	63.1 \pm 8.8	65.6 \pm 6.1	63.3 \pm 1.7
Random Forest	73.1 \pm 14.7	71.1 \pm 13.6	66.4 \pm 12.0	65.6 \pm 10.0	65.8 \pm 4.9

5.2 Data Quality Study on ABIDE Dataset

To evaluate the quality of our data collection, we performed a recent graph-based functional analysis approach [30] to both an existing graph-based brain connectivity dataset derived from ABIDE and our processed brain connectivity networks of the ABIDE. The approach in [30] (model version of CS-P1) calculates the average connectivity matrixes over the subjects in the contrast group and patient group, respectively. The difference matrix between the two average connectivity matrixes is called the contrast graph. Then CS-P1 finds the densest subgraph in the contrast graph, called the contrast dense subgraph, as the feature for classification. To make the classification fairer, we list two methods of finding the contrast dense subgraph for CS-P1 [30]:

- Method 1: using the whole dataset (all the subjects in both training and test sets) to extract the contrast dense subgraph. The results in [30] used this method.
- Method 2: using only the training set to extract the contrast dense subgraph.

We first applied the two methods of CS-P1 to the functional networks of different sub-groups of the ABIDE dataset: both the code and data were provided by the authors of [30]. The results using Method 1 (left part of Table 4) are generally comparable with the reported results in [30]: the reproduced accuracy is 3% lower than the claimed accuracy in the group of "Children", and 2% lower

in the group of "Eyesclosed"; the results on the other two groups are consistent. The accuracy results using Method 2 are much lower than the results using Method 1.

We then applied CS-P1 (the same code) on our functional networks of sub-groups of ABIDE dataset. The right part of Table 4 shows the result. Note that the subjects in different groups may overlap, besides, due to different data quality filtering procedures, there is a small difference in the number of subjects in each sub-group. It can be observed that from Method 1, the classification accuracy on our datasets is marginally better than those on the datasets provided by [30]; for Method 2, the classification accuracy of [30] on the dataset from [30] and that on our dataset are comparable. The results validate that the quality of the brain networks generated by our pipeline is up to the standard of those used in other studies.

Specifically, we first applied the approach of [30] (model version of CS-P1) to the functional networks of different sub-groups of the ABIDE dataset: both the code and data were provided by the authors of [30]. The results (left part of Table 4) are not entirely consistent with those reported in [30]: the reproduced accuracy is 6% lower than the claimed accuracy in the group of "Children", and 4% lower in the group of "Eyesclosed"; the results on the other two groups are consistent. Nonetheless, we have tried our best to reproduce the results using the parameters provided by the authors.

We then applied CS-P1 (the same code) on our functional networks of sub-groups of ABIDE dataset. The right part of Table 4 shows the result. Note that the subjects in different groups may overlap, besides, due to different data quality filtering procedures, there is a small difference in the number of subjects in each sub-group. It can be observed that the performance, i.e., the classification accuracy, of [30] on the dataset from [30] and that on our dataset are comparable. The results on our datasets are marginally better than those on the datasets provided by [30]. The results validate that the quality of the brain networks generated by our pipeline is up to the standard of those used in other studies.

Table 4: Results of CS-P1 [30] on the ABIDE dataset used in [30] and on our ABIDE dataset

Grouping	n	ABIDE used in [30]				Our ABIDE	
		Method 1 Accuracy [30]	Method 1 Reproduced accuracy	Method 2		Method 1 Reproduced accuracy	Method 2
Adolescents	237	72.0 \pm 7.0	71.4 \pm 3.7	64.9 \pm 7.8	259	72.2 \pm 5.5	68.3 \pm 3.1
Children	101	86.0 \pm 7.0	83.0 \pm 9.6	69.5 \pm 8.6	96	80.1 \pm 2.6	67.1 \pm 14.0
Eyesclosed	294	71.0 \pm 3.0	68.7 \pm 4.6	60.9 \pm 3.7	312	68.6 \pm 3.5	64.8 \pm 6.2
Male	838	63.0 \pm 1.0	63.5 \pm 2.3	60.4 \pm 5.1	873	65.3 \pm 2.1	62.7 \pm 4.0

6 Conclusions, Limitations, and Future Directions

We release a functional brain network collection to the public at a large scale. The collection originates from 5 raw MRI image sources well recognized in neuroscience, covers 3 neurodegenerative conditions, and totals to 2,642 subjects. Working with domain experts, we come up with a unified pipeline that converts raw fMRI and T1w images to brain networks. We tested the collection on baseline models and a recent graph-based model to demonstrate that the data quality is not compromised while at the same time providing the results as domain baselines. We hope that the release of this collection of brain networks, together with the complete code of the processing pipeline, will promote both the development of graph-based models and the clinical advancement in the diagnosis and early intervention of neurodegenerative diseases.

We identify two limitations of this study: (1) Though the current brain network collection contains 2,642 subjects, it may still be considered small when applied to certain machine learning models (e.g., deep learning models). Due to the high computational cost, we are not able to produce a larger collection for now but will make continuous efforts in enriching the collection, (2) The current collection focuses on extracting brain networks from a single modality, that is, the functional MRI images. Recently, neuroimaging data lean towards the direction of combining different modalities such as diffusion and functional MRI for further integrated explorations of brain functionalities. The fusion of functional MRI and diffusion MRI can encode information regarding integrated activities of the human brain. In the future, we plan to work on the processing pipeline of diffusion MRI images to make multi-modal brain networks publicly accessible to the research community.

Acknowledgments

This work is supported by MBIE Catalyst: Strategic Fund NZ-Singapore Data Science Research Programme UOAX2001 and National Research Foundation, Singapore under its Industry Alignment Fund – Pre-positioning (IAF-PP) Funding Initiative. Any opinions, findings and conclusions or recommendations expressed in this material are those of the author(s) and do not reflect the views of National Research Foundation, Singapore.

Neurocon data used in this article was obtained from the NEUROCON project (84/2012), financed by UEFISCDI.

ADNI data collection used in this article was funded by the ADNI (National Institutes of Health Grant U01 AG024904) and DOD ADNI (Department of Defense award number W81XWH-12-2-0012). ADNI is funded by the National Institute on Aging, the National Institute of Biomedical Imaging and Bioengineering, and through generous contributions from the following: AbbVie, Alzheimer’s Association; Alzheimer’s Drug Discovery Foundation; Araclon Biotech; BioClinica, Inc.; Biogen; Bristol-Myers Squibb Company; CereSpir, Inc.; Cogstate; Eisai Inc.; Elan Pharmaceuticals, Inc.; Eli Lilly and Company; EuroImmun; F. Hoffmann-La Roche Ltd and its affiliated company Genentech, Inc.; Fujirebio; GE Healthcare; IXICO Ltd.; Janssen Alzheimer Immunotherapy Research & Development, LLC.; Johnson & Johnson Pharmaceutical Research & Development LLC.; Lumosity; Lundbeck; Merck & Co., Inc.; Meso Scale Diagnostics, LLC.; NeuroRx Research; Neurotrack Technologies; Novartis Pharmaceuticals Corporation; Pfizer Inc.; Piramal Imaging; Servier; Takeda Pharmaceutical Company; and Transition Therapeutics. The Canadian Institutes of Health Research is providing funds to support ADNI clinical sites in Canada. Private sector contributions are facilitated by the Foundation for the National Institutes of Health (www.fnih.org). The grantee organization is the Northern California Institute for Research and Education, and the study is coordinated by the Alzheimer’s Therapeutic Research Institute at the University of Southern California. ADNI data are disseminated by the Laboratory for Neuro Imaging at the University of Southern California.

PPMI data collection used in this article were obtained from the PPMI database (<https://www.ppmi-info.org/accessdata-specimens/download-data>). PPMI – a public-private partnership – is funded by The Michael J. Fox Foundation for Parkinson’s Research and funding partners, including 4D Pharma, AbbVie Inc., AcureX Therapeutics, Allergan, Amathus Therapeutics, Aligning Science Across Parkinson’s (ASAP), Avid Radiopharmaceuticals, Bial Biotech, Biogen, BioLegend, Bristol Myers Squibb, Calico Life Sciences LLC, Celgene Corporation, DaCapo Brainscience, Denali Therapeutics, The Edmond J. Safra Foundation, Eli Lilly and Company, GE Healthcare, GlaxoSmithKline, Golub Capital, Handl Therapeutics, Insitro, Janssen Pharmaceuticals, Lundbeck, Merck & Co., Inc, Meso Scale Diagnostics, LLC, Neurocrine Biosciences, Pfizer Inc., Piramal Imaging, Prevail Therapeutics, F. Hoffmann-La Roche Ltd and its affiliated company Genentech Inc., Sanofi Genzyme, Servier, Takeda Pharmaceutical Company, Teva Neuroscience, Inc., UCB, Vanqua Bio, Verily Life Sciences, Voyager Therapeutics, Inc., Yumanity Therapeutics, Inc.. For up-to-date information on the study, visit www.ppmi-info.org.

References

- [1] A repository of benchmark graph datasets for graph classification. https://github.com/GRAND-Lab/graph_datasets.
- [2] A. Abraham, F. Pedregosa, M. Eickenberg, P. Gervais, A. Mueller, J. Kossaifi, A. Gramfort, B. Thirion, and G. Varoquaux. Machine learning for neuroimaging with scikit-learn. *Frontiers in neuroinformatics*, 8:14, 2014.
- [3] P. S. Aisen, R. C. Petersen, M. Donohue, M. W. Weiner, A. D. N. Initiative, et al. Alzheimer’s disease neuroimaging initiative 2 clinical core: progress and plans. *Alzheimer’s & Dementia*, 11(7):734–739, 2015.
- [4] P. S. Aisen, R. C. Petersen, M. C. Donohue, A. Gamst, R. Raman, R. G. Thomas, S. Walter, J. Q. Trojanowski, L. M. Shaw, L. A. Beckett, et al. Clinical core of the alzheimer’s disease neuroimaging initiative: progress and plans. *Alzheimer’s & Dementia*, 6(3):239–246, 2010.
- [5] B. B. Avants, N. J. Tustison, G. Song, P. A. Cook, A. Klein, and J. C. Gee. A reproducible evaluation of ants similarity metric performance in brain image registration. *Neuroimage*, 54(3):2033–2044, 2011.

- [6] L. Badea, M. Onu, T. Wu, A. Roceanu, and O. Bajenaru. Exploring the reproducibility of functional connectivity alterations in parkinson’s disease. *PLoS One*, 12(11):e0188196, 2017.
- [7] D. S. Bassett and O. Sporns. Network neuroscience. *Nature neuroscience*, 20(3):353–364, 2017.
- [8] L. A. Beckett, M. C. Donohue, C. Wang, P. Aisen, D. J. Harvey, N. Saito, A. D. N. Initiative, et al. The alzheimer’s disease neuroimaging initiative phase 2: Increasing the length, breadth, and depth of our understanding. *Alzheimer’s & Dementia*, 11(7):823–831, 2015.
- [9] I. Bilgen, G. Guvercin, and I. Rekik. Machine learning methods for brain network classification: Application to autism diagnosis using cortical morphological networks. *Journal of neuroscience methods*, 343:108799, 2020.
- [10] T. Bonald, N. de Lara, Q. Lutz, and B. Charpentier. Scikit-network: Graph analysis in python. *J. Mach. Learn. Res.*, 21(185):1–6, 2020.
- [11] S. Chen, Z. He, X. Han, X. He, R. Li, H. Zhu, D. Zhao, C. Dai, Y. Zhang, Z. Lu, et al. How big data and high-performance computing drive brain science. *Genomics, proteomics & bioinformatics*, 17(4):381–392, 2019.
- [12] R. W. Cox. Afni: Software for analysis and visualization of functional magnetic resonance neuroimages. *Computers and Biomedical Research*, 29(3):162–173, 1996.
- [13] C. Craddock, Y. Benhajali, C. Chu, F. Chouinard, A. Evans, A. Jakab, B. S. Khundrakpam, J. D. Lewis, Q. Li, M. Milham, et al. The neuro bureau preprocessing initiative: open sharing of preprocessed neuroimaging data and derivatives. *Frontiers in Neuroinformatics*, 7, 2013.
- [14] R. C. Craddock, G. A. James, P. E. Holtzheimer III, X. P. Hu, and H. S. Mayberg. A whole brain fmri atlas generated via spatially constrained spectral clustering. *Human brain mapping*, 33(8):1914–1928, 2012.
- [15] F. Errica, M. Podda, D. Bacciu, and A. Micheli. A fair comparison of graph neural networks for graph classification. *arXiv preprint arXiv:1912.09893*, 2019.
- [16] O. Esteban, C. J. Markiewicz, R. W. Blair, C. A. Moodie, A. I. Isik, A. Erramuzpe, J. D. Kent, M. Goncalves, E. DuPre, M. Snyder, et al. fmriprep: a robust preprocessing pipeline for functional mri. *Nature methods*, 16(1):111–116, 2019.
- [17] F. V. Farahani, W. Karwowski, and N. R. Lighthall. Application of graph theory for identifying connectivity patterns in human brain networks: a systematic review. *frontiers in Neuroscience*, 13:585, 2019.
- [18] B. Fischl. Freesurfer. *NeuroImage*, 62(2):774–781, 2012. 20 YEARS OF fMRI.
- [19] A. Fornito, A. Zalesky, and E. Bullmore. *Fundamentals of brain network analysis*. Academic Press, 2016.
- [20] S. Fortunato. Community detection in graphs. *Physics reports*, 486(3-5):75–174, 2010.
- [21] M. D. Fox and M. Greicius. Clinical applications of resting state functional connectivity. *Frontiers in systems neuroscience*, 4:19, 2010.
- [22] M. D. Fox, A. Z. Snyder, J. L. Vincent, M. Corbetta, D. C. Van Essen, and M. E. Raichle. The human brain is intrinsically organized into dynamic, anticorrelated functional networks. *Proceedings of the National Academy of Sciences*, 102(27):9673–9678, 2005.
- [23] M. D. Fox, D. Zhang, A. Z. Snyder, and M. E. Raichle. The global signal and observed anticorrelated resting state brain networks. *Journal of neurophysiology*, 101(6):3270–3283, 2009.
- [24] K. J. Gorgolewski, T. Auer, V. D. Calhoun, R. C. Craddock, S. Das, E. P. Duff, G. Flandin, S. S. Ghosh, T. Glatard, Y. O. Halchenko, et al. The brain imaging data structure, a format for organizing and describing outputs of neuroimaging experiments. *Scientific data*, 3(1):1–9, 2016.
- [25] M. Ingalhalikar, S. Shinde, A. Karmarkar, A. Rajan, D. Rangaprakash, and G. Deshpande. Functional connectivity-based prediction of autism on site harmonized abide dataset. *IEEE Transactions on Biomedical Engineering*, 68(12):3628–3637, 2021.
- [26] M. Jenkinson, C. F. Beckmann, T. E. Behrens, M. W. Woolrich, and S. M. Smith. Fsl. *NeuroImage*, 62(2):782–790, 2012. 20 YEARS OF fMRI.

- [27] C. Kamarajan, B. A. Ardekani, A. K. Pandey, S. Kinreich, G. Pandey, D. B. Chorlian, J. L. Meyers, J. Zhang, E. Bermudez, A. T. Stimus, et al. Random forest classification of alcohol use disorder using fmri functional connectivity, neuropsychological functioning, and impulsivity measures. *Brain sciences*, 10(2):115, 2020.
- [28] A. Kandel, H. Bunke, and M. Last. *Applied graph theory in computer vision and pattern recognition*. Springer Science & Business Media, 2007.
- [29] M. Koutrouli, E. Karatzas, D. Paez-Espino, and G. A. Pavlopoulos. A guide to conquer the biological network era using graph theory. *Frontiers in Bioengineering and Biotechnology*, page 34, 2020.
- [30] T. Lanciano, F. Bonchi, and A. Gionis. Explainable classification of brain networks via contrast subgraphs. In *Proceedings of the 26th ACM SIGKDD International Conference on Knowledge Discovery & Data Mining*, pages 3308–3318, 2020.
- [31] S. Li, H. Lei, F. Zhou, J. Gardezi, and B. Lei. Longitudinal and multi-modal data learning for parkinson’s disease diagnosis via stacked sparse auto-encoder. In *2019 IEEE 16th International Symposium on Biomedical Imaging (ISBI 2019)*, pages 384–387. IEEE, 2019.
- [32] X. Li, P. S. Morgan, J. Ashburner, J. Smith, and C. Rorden. The first step for neuroimaging data analysis: Dicom to nifti conversion. *Journal of neuroscience methods*, 264:47–56, 2016.
- [33] J. Liu, Y. Sheng, W. Lan, R. Guo, Y. Wang, and J. Wang. Improved asd classification using dynamic functional connectivity and multi-task feature selection. *Pattern Recognition Letters*, 138:82–87, 2020.
- [34] C. Lord, S. Risi, P. S. DiLavore, C. Shulman, A. Thurm, and A. Pickles. Autism from 2 to 9 years of age. *Archives of general psychiatry*, 63(6):694–701, 2006.
- [35] J. MacQueen et al. Some methods for classification and analysis of multivariate observations. In *Proceedings of the fifth Berkeley symposium on mathematical statistics and probability*, volume 1, pages 281–297. Oakland, CA, USA, 1967.
- [36] N. Makris, J. M. Goldstein, D. Kennedy, S. M. Hodge, V. S. Caviness, S. V. Faraone, M. T. Tsuang, and L. J. Seidman. Decreased volume of left and total anterior insular lobule in schizophrenia. *Schizophrenia research*, 83(2-3):155–171, 2006.
- [37] K. Marek, D. Jennings, S. Lasch, A. Siderowf, C. Tanner, T. Simuni, C. Coffey, K. Kieburtz, E. Flagg, S. Chowdhury, et al. The parkinson progression marker initiative (ppmi). *Progress in neurobiology*, 95(4):629–635, 2011.
- [38] C. Morris, N. M. Kriege, F. Bause, K. Kersting, P. Mutzel, and M. Neumann. Tudataset: A collection of benchmark datasets for learning with graphs. *arXiv preprint arXiv:2007.08663*, 2020.
- [39] S. Noble, D. Scheinost, E. S. Finn, X. Shen, X. Papademetris, S. C. McEwen, C. E. Bearden, J. Addington, B. Goodyear, K. S. Cadenehead, et al. Multisite reliability of mr-based functional connectivity. *Neuroimage*, 146:959–970, 2017.
- [40] S. Pan, J. Wu, X. Zhu, G. Long, and C. Zhang. Task sensitive feature exploration and learning for multitask graph classification. *IEEE transactions on cybernetics*, 47(3):744–758, 2016.
- [41] S. Parisot, S. I. Ktena, E. Ferrante, M. Lee, R. G. Moreno, B. Glocker, and D. Rueckert. Spectral graph convolutions for population-based disease prediction. In *International conference on medical image computing and computer-assisted intervention*, pages 177–185. Springer, 2017.
- [42] F. Pedregosa, G. Varoquaux, A. Gramfort, V. Michel, B. Thirion, O. Grisel, M. Blondel, P. Prettenhofer, R. Weiss, V. Dubourg, J. Vanderplas, A. Passos, D. Cournapeau, M. Brucher, M. Perrot, and E. Duchesnay. Scikit-learn: Machine learning in Python. *Journal of Machine Learning Research*, 12:2825–2830, 2011.
- [43] J. B. Pereira, D. Aarsland, C. E. Ginestet, A. V. Lebedev, L.-O. Wahlund, A. Simmons, G. Volpe, and E. Westman. Aberrant cerebral network topology and mild cognitive impairment in early parkinson’s disease. *Human brain mapping*, 36(8):2980–2995, 2015.
- [44] D. Polšek, T. Jagatic, M. Cepanec, P. Hof, and G. Šimić. Recent developments in neuropathology of autism spectrum disorders. *Translational neuroscience*, 2(3):256–264, 2011.
- [45] Z. Rakhimberdina, X. Liu, and T. Murata. Population graph-based multi-model ensemble method for diagnosing autism spectrum disorder. *Sensors*, 20(21):6001, 2020.

- [46] A. Schaefer, R. Kong, E. M. Gordon, T. O. Laumann, X.-N. Zuo, A. J. Holmes, S. B. Eickhoff, and B. T. Yeo. Local-global parcellation of the human cerebral cortex from intrinsic functional connectivity mri. *Cerebral cortex*, 28(9):3095–3114, 2018.
- [47] L. Tang and H. Liu. Graph mining applications to social network analysis. In *Managing and mining graph data*, pages 487–513. Springer, 2010.
- [48] N. Tzourio-Mazoyer, B. Landeau, D. Papathanassiou, F. Crivello, O. Etard, N. Delcroix, B. Mazoyer, and M. Joliot. Automated anatomical labeling of activations in spm using a macroscopic anatomical parcellation of the mni mri single-subject brain. *Neuroimage*, 15(1):273–289, 2002.
- [49] J. H. Ward Jr. Hierarchical grouping to optimize an objective function. *Journal of the American statistical association*, 58(301):236–244, 1963.
- [50] M. W. Weiner, D. P. Veitch, P. S. Aisen, L. A. Beckett, N. J. Cairns, R. C. Green, D. Harvey, C. R. Jack Jr, W. Jagust, J. C. Morris, et al. The alzheimer’s disease neuroimaging initiative 3: Continued innovation for clinical trial improvement. *Alzheimer’s & Dementia*, 13(5):561–571, 2017.
- [51] C. Yan and Y. Zang. Dparsf: a matlab toolbox for" pipeline" data analysis of resting-state fmri. *Frontiers in systems neuroscience*, page 13, 2010.
- [52] M. Zhang and Y. Chen. Link prediction based on graph neural networks. *Advances in neural information processing systems*, 31, 2018.
- [53] X. Zhang, B. Hu, X. Ma, and L. Xu. Resting-state whole-brain functional connectivity networks for mci classification using l2-regularized logistic regression. *IEEE transactions on nanobioscience*, 14(2):237–247, 2015.
- [54] X. Zhang, J. Huang, Y. Yang, X. He, R. Liu, and N. Zhong. Applying python in brain science education. In *2019 International Joint Conference on Information, Media and Engineering (IJCIME)*, pages 396–400. IEEE, 2019.
- [55] X. Zhou, S. Wang, W. Xu, G. Ji, P. Phillips, P. Sun, and Y. Zhang. Detection of pathological brain in mri scanning based on wavelet-entropy and naive bayes classifier. In *International conference on bioinformatics and biomedical engineering*, pages 201–209. Springer, 2015.

A Appendix

A.1 Dataset-related Details

A.1.1 Dataset Documentation

We provide a datasheet that documents this data collection (in the Supplementary materials).

A.1.2 Access Link and Data Repositories

The brain network datasets can be accessed at: <https://doi.org/10.17608/k6.auckland.21397377>. *A public DOI assigned through Figshare will be used with the exception of brain networks created with neuroimages from ADNI. ADNI has requested that derived data should be hosted in the same data repository as the original imaging data, LONI IDA.*

We have a Github repository at <https://github.com/bna-data-analysis/extract-brain-network> which includes all our preprocessing codes and a demo on how to convert a raw fMRI image to a brain network in a step-by-step manner with sample input images from a subject in TaoWu.

Figshare (<https://www.figshare.com>) is a citable, shareable, and discoverable open data repository used by many educational institutions around the world, including ours. Figshare fits the many requirements of NeurIPS, including long term preservations of the data, access to a persistent identifier (an assigned DOI), and clear licensing and data standards.

LONI IDA (<https://ida.loni.usc.edu/>) is a global leader in neuroscience data management and informatics solutions that facilitate data preservation, exploration and sharing. LONI hosts most of the major multi-site neuroimaging studies in the world and is the domain standard for obtaining neuroimages from large-scale studies.

A.1.3 Author Statement

As authors, we confirm that we bear all responsibility in case of any violation of rights during the collection of the data or other work, and will take appropriate action when needed, to remove data with such issues.

A.1.4 License of our Brain Network Datasets

CC BY-NC-SA 4.0

A.1.5 Consent Process for Neuroimages

ABIDE, TaoWu, and Neurocon all follow Creative Common licenses and their source neuroimages are open use. For ADNI and PPMI we have followed their policies (Data Usage and Publication Policy) on how to use and publish derived data and where appropriate, we have submitted our manuscripts for permission to publish. ADNI has additionally requested that the derived data should be hosted in the same data repository LONI IDA (which we will comply with). PPMI has also confirmed that it is acceptable to publish derived work from their neuroimages. Both required proper acknowledgements of the entity and their funders in the paper, which we have included.

A.1.6 Computing Resources Used for Preprocessing

As stated in the main paper, fMRIPrep is computationally expensive. In our case, one run on one subject of fMRIPrep (with surface reconstruction enabled) using 8 threads on an Intel(R) Core(TM) i9-10940X CPU @ 3.30GHz takes on average 4-5 hours. Preprocessing of all data sources was split between two sites running on different internal cluster configurations. We are currently storing approximately 5 TB of data on these clusters, including the original neuroimages, preprocessed neuroimages, and our derived brain network data.

Site 1 cluster:

1. 3x Intel(R) Core(TM) i9-10940X CPU @ 3.30GHz

2. 1x Intel(R) Xeon(R) CPU ES-4020 v2 @ 2.60GHz

Site 2 cluster:

1. 5x Intel(R) Xeon(R) Silver 4314 CPU @ 2.40GHz
2. 1x Intel(R) Xeon(R) Gold 6230 CPU @ 2.10GHz

A.2 Experiment-related Details

A.2.1 Code

The code we used to run our entire pipeline and baseline experiments can be accessed on our Github: <https://github.com/bna-data-analysis/extract-brain-network>.

A.2.2 Parameters

As stated in the main paper we used scikit-learn for all our implementations and here we provide the full list of parameters (including those we used to Grid Search).

LogisticRegression(*penalty*=(*'l1'*, *'l2'*, *'elasticnet'*, *'none'*), *dual*=*False*, *tol*=*0.0001*, *C*=*1.0*, *fit_intercept*=*True*, *intercept_scaling*=*1*, *class_weight*=*None*, *random_state*=*None*, *solver*=*'lbfgs'*, *max_iter*=*1000000*, *multi_class*=*'auto'*, *verbose*=*0*, *warm_start*=*False*, *n_jobs*=*None*, *l1_ratio*=*None*)

GaussianNB(*priors*=*None*, *var_smoothing*=*1e-09*)

SVC(*C*=(*0.1*, *1*, *10*), *kernel*=(*'rbf'*, *'linear'*, *'poly'*, *'sigmoid'*), *degree*=*3*, *gamma*=(*'auto'*, *'scale'*), *coef0*=*0.0*, *shrinking*=*True*, *probability*=*False*, *tol*=*0.001*, *cache_size*=*200*, *class_weight*=*None*, *verbose*=*False*, *max_iter*=*-1*, *decision_function_shape*=*'ovr'*, *break_ties*=*False*, *random_state*=*None*)

KNeighborsClassifier(*n_neighbors*=(*3*, *4*, *5*, *6*), *weights*=(*'uniform'*, *'distance'*), *algorithm*=*'auto'*, *leaf_size*=*30*, *p*=(*1*, *2*), *metric*=*'minkowski'*, *metric_params*=*None*, *n_jobs*=*None*)

RandomForestClassifier(*n_estimators*=(*50*, *100*, *150*, *200*), *criterion*=(*'gini'*, *'entropy'*), *max_depth*=(*2*, *3*, *4*, *5*), *min_samples_split*=*2*, *min_samples_leaf*=*1*, *min_weight_fraction_leaf*=*0.0*, *max_features*=*'sqrt'*, *max_leaf_nodes*=*None*, *min_impurity_decrease*=*0.0*, *bootstrap*=*True*, *oob_score*=*False*, *n_jobs*=*None*, *random_state*=*0*, *verbose*=*0*, *warm_start*=*False*, *class_weight*=*None*, *ccp_alpha*=*0.0*, *max_samples*=*None*)

A.2.3 Computing Resources Used for Baselines

Experiments on baselines were performed on the internal cluster at site 2 (stated above).

A.2.4 Connectivity Measure Comparison on TaoWu

Table 5: Connectivity Measure Comparison - Classification Accuracy (mean \pm standard deviation)

	TaoWu - AAL116			
	Correlation	Covariance	Partial Correlation	Precision
Logistic Regression	82.5 \pm 12.7	82.5 \pm 12.7	62.5 \pm 5.0	65.0 \pm 12.2
Naïve Bayes	61.5 \pm 19.0	61.5 \pm 19.0	45.0 \pm 16.2	43.5 \pm 16.2
SVC	85.0 \pm 9.4	85.0 \pm 9.4	65.0 \pm 20.0	65.0 \pm 14.6
kNN	60.0 \pm 21.5	60.0 \pm 14.6	52.5 \pm 5.0	57.5 \pm 6.1
Random Forest	72.5 \pm 12.2	70.0 \pm 10.0	65.0 \pm 18.4	62.5 \pm 7.9

A.2.5 Accuracy Comparison of Sklearn Default Parameters vs. Grid Searching for the Best Model

Table 6: Classification Accuracy (mean \pm standard deviation)

ABIDE		
AAL	Original	With Model Selection
Logistic Regression	62.9 \pm 3.5	63.9 \pm 3.3
Naïve Bayes	60.7 \pm 5.0	60.7 \pm 5.0
SVC	66.3 \pm 5.3	66.5 \pm 3.0
kNN	60.0 \pm 2.8	60.6 \pm 1.7
Random Forest	60.4 \pm 4.0	64.1 \pm 4.0
ADNI		
AAL	Original	With Model Selection
Logistic Regression	75.6 \pm 2.3	74.9 \pm 2.2
Naïve Bayes	62.1 \pm 3.1	62.1 \pm 3.1
SVC	62.2 \pm 2.7	76.6 \pm 1.7
kNN	62.5 \pm 3.4	67.5 \pm 3.5
Random Forest	62.6 \pm 2.9	66.9 \pm 1.3
PPMI		
AAL	Original	With Model Selection
Logistic Regression	53.6 \pm 5.6	56.4 \pm 2.1
Naïve Bayes	61.0 \pm 7.1	61.0 \pm 7.1
SVC	61.7 \pm 7.1	65.1 \pm 3.3
kNN	51.0 \pm 7.1	54.5 \pm 3.4
Random Forest	64.5 \pm 6.2	66.1 \pm 2.5
TaoWu		
AAL	Original	With Model Selection
Logistic Regression	72.5 \pm 15.8	82.5 \pm 12.7
Naïve Bayes	61.5 \pm 19.0	61.5 \pm 19.0
SVC	44.0 \pm 18.7	85.0 \pm 9.4
kNN	52.0 \pm 15.7	60.0 \pm 21.5
Random Forest	52.5 \pm 19.8	72.5 \pm 12.2
Neurocon		
AAL	Original	With Model Selection
Logistic Regression	57.8 \pm 13.7	63.1 \pm 11.8
Naïve Bayes	60.0 \pm 14.1	60.0 \pm 14.1
SVC	60.9 \pm 12.6	65.8 \pm 4.9
kNN	52.9 \pm 13.1	65.6 \pm 6.1
Random Forest	62.2 \pm 14.7	73.1 \pm 14.7